Intranasal Administration of Extracellular Vesicles Derived from Human Teeth Stem Cells Improves Motor Symptoms and Normalizes Tyrosine Hydroxylase Expression in the Substantia Nigra and Striatum of the 6-Hydroxydopamine-Treated Rats

Karīna Narbute,[a] Vladimirs Pilipenko,[a] Jolanta Pupure,[a] Zane Dzirkale,[a] Ugnė Jonavičė,[b] Virginijus Tunaitis,[b] Karolina Kriaučiūnaitė,[b] Akvilė Jarmalavičiūtė,[b] Baiba Jansone,[a] Vija Klуša,[a] Augustas Pivoriūnas [b]

Key Words. Adult stem cells • Animal models • Cell signaling • Cellular therapy • Differentiation • Parkinson's disease • Mesenchymal stem cells

[a]Department of Pharmacology, Faculty of Medicine, University of Latvia, Riga, Latvia; [b]Department of Stem Cell Biology, State Research Institute Centre for Innovative Medicine, Vilnius, Lithuania

Correspondence: Augustas Pivoriūnas, M.D., Ph.D., Department of Stem Cell Biology, State Research Institute Centre for Innovative Medicine, Santariškių 5, 08406 Vilnius, Lithuania. Telephone: +37052628413; e-mail: augustas. pivoriunas@imcentras.lt

Abstract

Parkinson's disease (PD) is the second most common neurodegenerative disorder affecting millions of people worldwide. At present, there is no effective cure for PD; treatments are symptomatic and do not halt progression of neurodegeneration. Extracellular vesicles (EVs) can cross the blood–brain barrier and represent promising alternative to the classical treatment strategies. In the present study, we examined therapeutic effects of intranasal administration of EVs derived from human exfoliated deciduous teeth stem cells (SHEDs) on unilateral 6-hydroxydopamine (6-OHDA) medial forebrain bundle (MFB) rat model of PD. CatWalk gait tests revealed that EVs effectively suppressed 6-OHDA-induced gait impairments. All tested gait parameters (stand, stride length, step cycle, and duty cycle) were significantly improved in EV-treated animals when compared with 6-OHDA-lesion group rats. Furthermore, EVs slowed down numbers of 6-OHDA-induced contralateral rotations in apomorphine test. Improvements in motor function correlated with normalization of tyrosine hydroxylase expression in the striatum and substantia nigra. In conclusion, we demonstrated, for the first time, the therapeutic efficacy of intranasal administration of EVs derived from SHEDs in a rat model of PD induced by 6-OHDA intra-MFB lesion. Our findings could be potentially exploited for the development of new treatment strategies against PD. STEM CELLS TRANSLATIONAL MEDICINE 2019;8:490–499

Significance Statement

Extracellular vesicles (EVs) derived from human exfoliated deciduous teeth stem cells were administered intranasally in model-rats of Parkinson's disease (PD), obtained by unilateral injection of 6-hydroxydopamine (6-OHDA) into the medial forebrain bundle. It was demonstrated that EVs can effectively suppress 6-OHDA-induced gait impairments and normalize tyrosine hydroxylase expression in the striatum and in the substantia nigra of experimental rats. To the authors' knowledge, this is the first report showing the therapeutic efficacy of intranasally administered EVs in the unilateral 6-OHDA rat model of PD. The findings may be useful for the development of new treatment strategies against PD.

Introduction

Parkinson's disease (PD) is the second most common neurodegenerative disorder affecting more than 1% of the population aged over 65 years and nearly 5% of those aged over 80 years [1]. At present, there is no effective cure for PD; treatments are symptomatic and they do not target neurodegeneration [2]. Stem cell research has

the potential to significantly impact the development of disease-modifying treatments for PD. Preclinical studies demonstrated that transplantation of pluripotent stem cell-derived dopaminergic neurons improved specific symptoms in animal models of PD [3, 4], and clinical trials are about to begin [5]. Nonetheless, alternative therapies with noninvasive administration procedures remain to be found. Deployment of

extracellular vesicles (EVs), which carry multiple proteins, RNAs, lipids, and metabolites [6, 7] represent promising alternative to the classical treatment strategies. Usage of EVs has several advantages from a therapeutic perspective. First, they can cross blood–brain barrier and thus can be delivered into the brain without complex neurosurgical interventions [8, 9]. Second, EVs are safer because of reduced risks associated with transplantation of cells, such as massive loss of transplanted cells, malignant transformation, or immune rejection. Third, EVs are relatively simple, stable, and controllable systems, being thus suitable for the large-scale clinical manufacturing [10]. Preclinical studies demonstrated that intranasal delivery of EVs from the bone marrow mesenchymal stem cells (MSCs) prevented abnormal neurogenesis and memory dysfunction after induction of status epilepticus in mice [11]. Treatment with EVs also suppressed neuroinflammation and reduced cognitive impairments after traumatic brain injury in mice [12]. Intranasal administration of catalase-loaded exosomes provided significant neuroprotective effects in PD model by safeguarding substantia nigra (SN) pars compacta neurons from oxidative stress-induced cell death [13], while curcumin-encapsulated exosomes suppressed IL-6 and TNF-α expression in LPS-induced septic shock model animals [14].

In the present study, we used EVs derived from stem cells from the dental pulp of human exfoliated deciduous teeth (SHEDs). These cells originate from the peripheral nerve-associated glia [15] and in contrast to the MSC-like cells derived from other mesodermal tissues have unique neurogenic properties [16, 17]. Moreover, SHEDs were efficiently differentiated into dopaminergic neuron-like cells [18] and Schwann cells [19]. Our previous in vitro studies revealed that EVs derived from SHEDs can suppress 6-hydroxydopamine (6-OHDA)-induced apoptosis of human dopaminergic neurons [20].

Here, we examined therapeutic effects of intranasal (i.n.) administration of EVs on rat model of PD obtained by unilateral 6-OHDA injection into the medial forebrain bundle (MFB). Our aim was to accomplish a severe, but not full lesion in the nigro-striatal structures, to study whether EVs could be used for slowing down progression of the disease. We started daily EVs treatments from day 8 after 6-OHDA injection and continued it for 15 days. Motor functions (gait) and tyrosine hydroxylase (TH) expression in the nigro-striatal structures were then assessed. Our study demonstrates that EVs can effectively ameliorate 6-OHDA-induced gait impairments and decreased TH expression in the striatum and in the SN of experimental rats. To the best of our knowledge, this is the first report showing the therapeutic capacity of intranasally administered EVs in the 6-OHDA rat model of PD. Our findings may be useful for the development of new treatment strategies against PD.

MATERIALS AND METHODS

Chemicals and Antibodies

The following chemicals were purchased from Sigma-Aldrich, St. Louis, MO: Apomorphine (A4393-1G), 3,3′-diaminobenzidine (DAB, D5905), ExtrAvidin Peroxidase Staining Kit (EXTRA2), Bovine serum albumine (BSA, A2058) and anti-TH antibody (T2928), Triton X-100 (X100), and 6-OHDA (H116). Antibodies against Syntenin-1, MFG-E8, and LGR5 were purchased from Santa Cruz Biotechnology (Santa Cruz, CA). Anti-HSP 70 antibody was from BD Transduction Laboratories (Becton, Dickinson and Company, Franklin Lakes, NY).

Artificial cerebrospinal fluid (aCSF) was prepared ex tempore. Apomorphine was dissolved in saline prior to the injection.

Isolation and Culture of SHEDs

Cells were obtained from human exfoliated deciduous teeth of a child, whose parents had signed an informed consent. Material was collected under the approval of the Lithuanian Bioethics committee (Nr. 6B-08-173). Briefly, the collected tooth was washed in phosphate-buffered saline (PBS) and incubated in low glucose (LG; 1 mg/ml) Dulbecco's modified Eagle's medium (DMEM; Biochrom) with 200 U/ml penicillin, 200 μg/ml streptomycin and 2.5 μg/ml of amphotericin B (all from Biochrom, Berlin, Germany). Pulp tissue was scraped out and placed in collagenase type I (Gibco, Invitrogen, Grand Island, NY) solution, the latter of which consisted of 0.2% collagenase in DMEM with 1% bovine serum albumin (BSA; Applichem, Darmstadt, Germany), 100 U/ml penicillin and 100 μg/ml streptomycin and incubated for 1 hour at 37°C in an orbital shaker platform. After digestion, the cell suspension was diluted in PBS and centrifuged at 250g for 5 minutes. The supernatant was discarded, cells resuspended in LG DMEM supplemented with 10% fetal bovine serum (Gibco), glutamine and antibiotics and plated. Cultures were maintained at 37°C in a humidified atmosphere containing 5% CO_2.

For the isolation of EVs SHEDs from third to fifth passages were grown until the cultures reached subconfluence, then standard medium was changed to the serum-free medium MSC NutriStem XF (Biological Industries, Kibbutz Beit Haemek, Israel).

Isolation of EVs

Isolation of EVs was performed using differential centrifugation according to the described protocol [20] with some modifications. All centrifugation steps were performed at 4°C. Supernatants collected from SHEDs cultivated in serum-free medium MSC NutriStem XF (Biological Industries) were centrifuged successively at increasing speeds (300g for 10 minutes, 2,000g for 10 minutes, then at 20,000g for 30 minutes). The final supernatants were ultracentrifuged at 100,000g for 70 minutes in Sorvall LYNX 6000 ultracentrifuge, with rotor T29-8x50 in oak ridge centrifuge tubes with sealing caps (all from Thermo Fisher Scientific, Rochester, NY), then the pellets were washed in 40 ml PBS and ultracentrifuged again at 100,000g for 70 minutes. Final pellets of EVs (exosomal fraction) were resuspended in sterile PBS and stored at −20°C.

Nanoparticle tracking analysis (NTA) was performed with NanoSight LM10 (Malvern Panalytical, Malvern, UK). NTA analyses revealed that EV fractions contained vesicles of approximately 100 nm in size (Fig. 1A–1C). EV fractions were also positive for the characteristic markers of exosomes (Syntenin 1, HSP70, MFG-E8; Fig. 1C). All preparations of EVs were derived from the same SHED line. Before the experiment, all EV preparations were pooled and divided into the single dose aliquots (10 μl). According to the NTA measurements single dose of EV contained 2.85×10^8 vesicles.

Animals

Male Wistar rats (280 $\pm$ 20g) were obtained from the State Research Institute Centre for Innovative Medicine Laboratory animals breeding house, Vilnius, Lithuania. Experiments on animals were performed under the approval of the Lithuanian Laboratory Use Ethics Committee under the State Food and Veterinary service (No. G2-51). All efforts were made to minimize
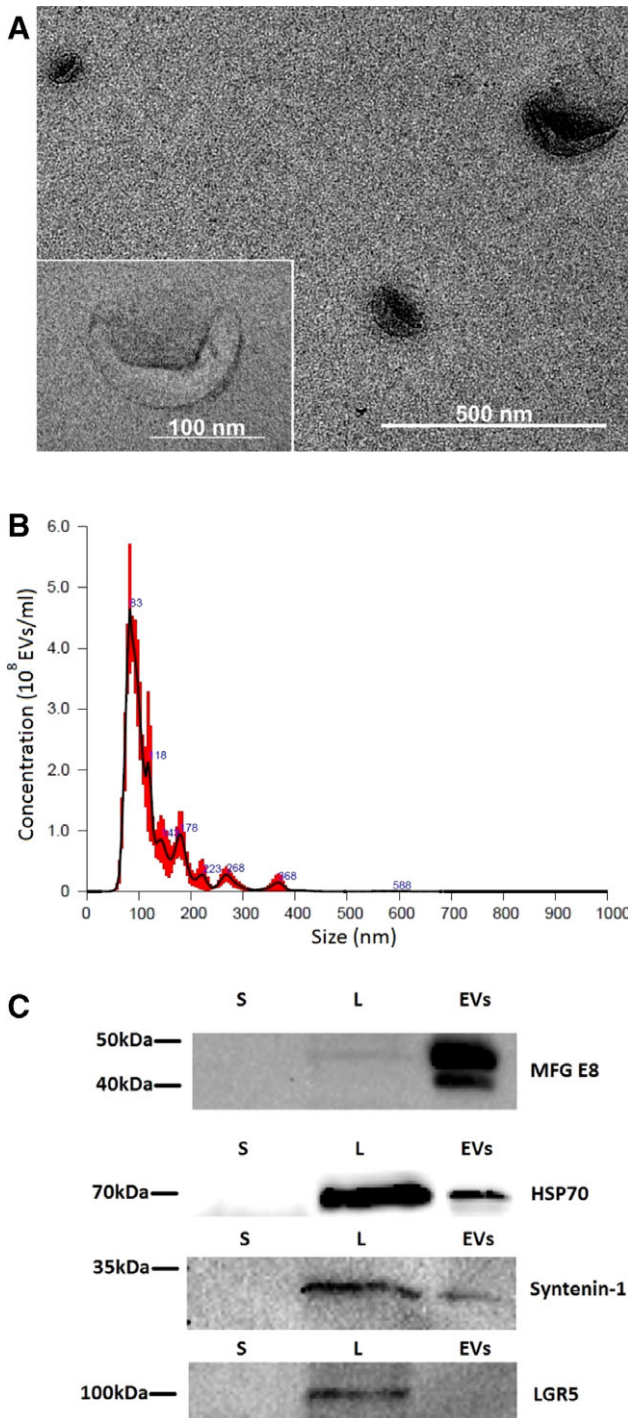
Figure 1. Characterization of extracellular vesicles (EVs) isolated from stem cells from the dental pulp of human exfoliated deciduous teeth (SHEDs). **(A):** Transmission electron microscopy of EVs isolated from SHEDs (×30,000 magnification). A magnified image of EV is shown on the left panel (×120,000 magnification). **(B):** Determination of the concentration and particle size of EVs derived from SHEDs. Nanoparticle tracking analysis was performed with NanoSight LM10 instrument (Malvern Panalytical). Size distribution of the EVs was around 100 nm. **(C):** Samples from supernatants (S), cell lysates (L), and EV fractions (EVs) were subjected to electrophoresis, blotted and the membrane was probed with antibodies against EV markers (HSP70, MFG-E8, syntenin-1), or LGR5 as a negative control. Bands were visualized by incubation with appropriate horseradish peroxidase-conjugated secondary antibodies and chemiluminescence substrate.

animal suffering and reduce the number of animals used. The experiments were conducted in accordance with the EU Directive 2010/63/EU and local laws and policies on the protection of animals used for scientific purposes. The animals were housed in a controlled laboratory environment (temperature $22°C \pm 2°C$, humidity 55%–65%, 12-hour light/dark cycle), five animals per polypropylene cage with food and water provided ad libitum.

Experimental Design (In Vivo)

Experimental design is shown in Figure 2. The rats were randomly divided into four groups ($n = 8$).

1. aCSF (intra-MFB) + PBS (i.n.);
2. aCSF (intra-MFB) + EVs (i.n.);
3. 6-OHDA (intra-MFB) + PBS (i.n.);
4. 6-OHDA (intra-MFB) + EVs (i.n.).

EVs were administered using a small pipette. Solution of 5 µl was administered in each nostril with 2 minutes interval. Each daily dose contained 2.85×10^8 vesicles/10 µl.

Overall, during 15 days each rat received a total of 180 µl EV solution containing approximately 43×10^8 EVs. After brain removal, immunohistochemical assessments were performed.

Unilateral 6-OHDA Lesion

Thirty minutes before the induction of general anesthesia, rats received imipramine (20 mg/kg) to protect adrenergic neurons against the development of 6-OHDA-induced lesions. The animals were anesthetized with isoflurane (3%–3.5% for induction and 2% for maintenance) and placed on a stereotaxic frame (Stoelting Inc.). On experimental day 15, unilateral 6-OHDA (20 µg in 3 µl of 0.2% ascorbic acid) or aCSF (control, 3 µl) were injected intra-MFB during stereotaxic surgery using the following coordinates: −2.2 mm anteroposterior, +1.5 mm mediolateral, and −8.0 mm dorsoventral relative to the bregma, using a 27-gauge needle attached to a 50 µl microsyringe (Hamilton). Injection flow was controlled using an electronic pump (World Precision Instruments, Sarasota, FL) at a rate of 1 µl per min. The microsyringe needle was left in the injection site for 5 minutes after each injection to avoid liquid reflux.

Apomorphine-Induced Rotation Behavior

On experimental day 23, apomorphine-induced rotational behavior was used to evaluate the dopaminergic neuron lesion induced by 6-OHDA. Apomorphine was dissolved in saline and injected subcutaneously at the dose of 0.2 mg/kg. After 5 minutes, the rotations were monitored for 30 minutes. The number of contralateral rotations (to the nonlesioned side) was recorded by examiner blinded to the groups.

CatWalk Gait Test

The CatWalk XT quantitative gait analysis system (Noldus, Wageningen, The Netherlands) is a nonintrusive, accurate tool to determine gait ability in rodents. This method is described elsewhere [21, 22]. In brief, it is based on rodent voluntary movement through an enclosed 1.3 m long glass walkway that is illuminated with green fluorescent lighting the walkway from the side and reflecting internally after the rodent comes in contact with the glass floor. High-speed video camera was located under the walkway and was used to obtain footprint images. The rats were trained twice: 7 days prior to 6-OHDA
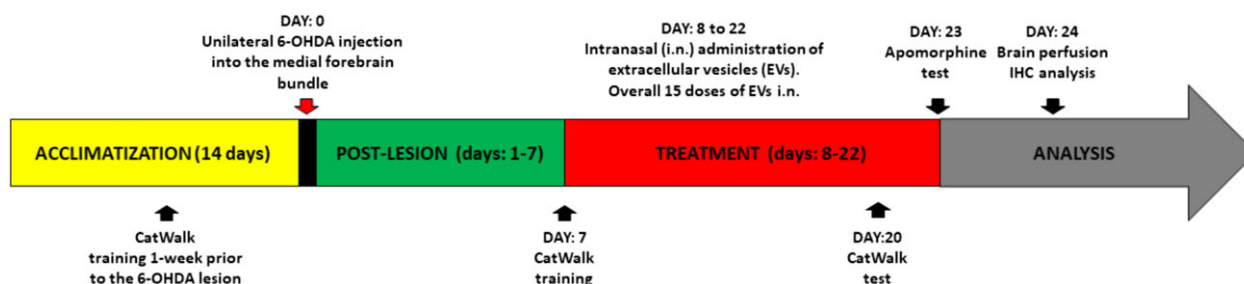
Figure 2. Experimental design of a study.

injection and on experimental day 7. Before each training session, the animals were placed on the walkway and allowed to habituate for 2 minutes. Testing was performed on experimental day 20 between 11:00 and 14:00, at least 1 hour after intranasal EVs administration. Testing was successful if the animal crossed the walkway without stopping and at least 3–4 each paw placements were recorded. Three complete runs across the walkway were recorded for each animal. CatWalk XT software was used to automatically analyze the video images of the runs. Data analysis was performed with a threshold value set at 40 arbitrary units (range 0–225) per pixel. The following parameters were analyzed according to [21, 23]: temporal (stand duration), spatial parameters attributed to individual paws (duty cycle, %), relative spatial relationships between paws (stride length) and interlimb coordination (step cycle). Duty cycle is calculated according to the formula: stand/(stand + swing) × 100% and it represents the stand as a percentage of step cycle.

Immunohistochemistry

The next day after the apomorphine rotation test, rats were deeply anesthetized with a ketamine/xylazine (100/10 mg/kg i.p.) mixture, transcardially perfused with ice-cold saline and fixed with cold 4% paraformaldehyde (PFA) solution. The brains were removed and postfixed in 4% PFA for 24 hours. After fixation, the brains were placed in 30% sucrose-containing solution for 48 hours for cryoprotection and subsequently placed in an antifreeze solution.

For each brain, 30 μm thick coronal slices were obtained using a cryotome at −23°C (CM1850, Leica Biosystems, Nussloch, Germany): 6 sections each from both the corpus striatum (AP plane −0.36 mm to −0.60 mm from bregma) and SN (AP plane −4.80 mm to −5.04 mm from bregma). The slices were incubated in citrate buffer (pH 6.0) at high temperature (95°C) for 10 minutes to improve antigen retrieval, subsequently cooled to room temperature and blocked with a 5% BSA solution for 30 minutes to decrease backstain formation. Free-floating sections were then stained with the corresponding primary antibody (1:1,000). The sections were transferred to a solution containing the primary antibody in PBS with 0.5% Triton X-100 (PBS-T). After 18 hour incubation, the sections were rinsed three times with PBS-T and transferred to a solution containing the secondary antibody (dilution 1:500). After 1.5 hour incubation with the secondary antibody, the sections were rinsed three times with PBS-T and transferred to PBS-T containing mouse ExtrAvidin Peroxidase (1:1,000) for 1.5 hour. After rinsing with PBS-T, the sections were incubated with PBS containing DAB, 30% H_2O_2 and nickel ammonium sulphate for 1 minute. All stained sections were mounted on slides (3 sections on each slide) and coverslipped using DPX mountant for histology. In
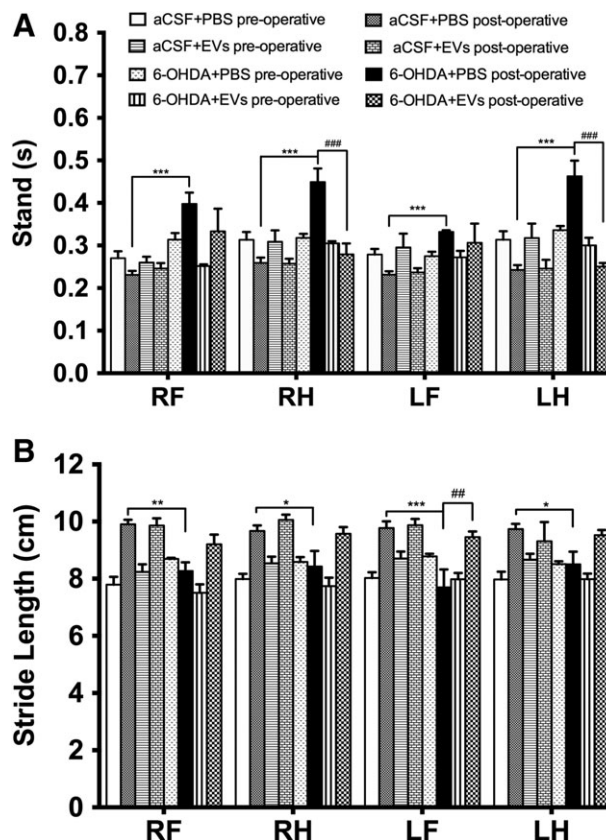

Figure 3. Effects of intranasally administered extracellular vesicles on rat stand and stride length in the CatWalk test in day 20 after medial forebrain bundle lesion. Stand **(A)**, stride length **(B)**. Data represent mean ± SEM values. One-way ANOVA followed by Fisher's LSD post-test. RF, right front paw; RH, right hind paw; LF, left front paw; LH, left hind paw. *, $p \leq .05$; **, $p \leq .01$; ***, $p \leq .001$ versus aCSF+PBS postoperative; ##, $p \leq .01$; ###, $p \leq .001$ versus 6-OHDA +PBS postoperative.

order to obtain similar staining, the sections from all groups were always stained simultaneously in the same tray. Optical density of protein staining was expressed in arbitrary units (a.u.).

Quantification

The mounted brain sections were scanned using a Pannoramic Midi II Scanner (3DHISTECH, Budapest, Hungary) at ×200 magnification. The optical density of neuronal (TH) staining was determined in the corpus striatum and SN regions. An observer blinded to the treatment of the animals performed all measurements in duplicate using the ImageJ software.
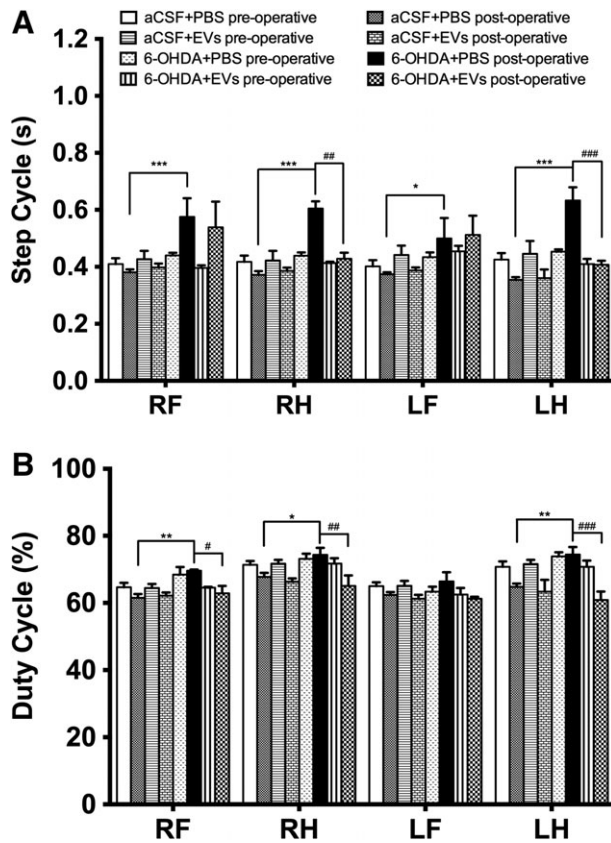
A

Legend:
- □ aCSF+PBS pre-operative
- ▦ aCSF+EVs pre-operative
- ▨ 6-OHDA+PBS pre-operative
- ▥ 6-OHDA+EVs pre-operative
- ▨ aCSF+PBS post-operative
- ▦ aCSF+EVs post-operative
- ■ 6-OHDA+PBS post-operative
- ▨ 6-OHDA+EVs post-operative

B

Figure 4. Effects of intranasally administered extracellular vesicles on step cycle and duty cycle in the CatWalk test in day 20 after medial forebrain bundle lesion: step cycle **(A)** and duty cycle **(B)**. Data represent mean ± SEM values. One-way ANOVA followed by Fisher's LSD post-test. RF, right front paw; RH, right hind paw; LF, left front paw; LH, left hind paw. *, $p \le .05$; **, $p \le .01$; ***, $p \le .001$ versus aCSF+PBS postoperative; ##, $p \le .01$; ###, $p \le .001$ versus 6-OHDA+PBS postoperative.

Transmission Electron Microscopy of EVs

EV samples for transmission electron microscopy have been prepared according to the previously published protocol [24] with some modifications. Briefly, EVs in PBS were fixed by adding 4% PFA to a final concentration of 2% and incubated for 40 minutes on ice. To absorb the sample, Formvar–carbon coated copper grid was floated on a 10 μl drop of EV suspension for 20 minutes at room temperature. After adsorption the grid was washed for 2 minutes at room temperature in a 100 μl drop of PBS. Then the grid was incubated in a 50 μl drop of 1% glutaraldehyde for 5 minutes at room temperature. Afterward 8 washing steps were performed (2 minutes for each) by transferring grid from one drop of distilled water to another. Samples were contrasted on a 50 μl drop of 2% neutral uranyl acetate for 5 minutes at room temperature in the dark. Afterward the grids were incubated on a 50 μl drop of 2% methylcellulose/0.4% uranyl acetate for 10 minutes on ice in the dark. In the end grids were taken by stainless steel loop and excess of liquid removed by filter paper. Then the grids on the same loop were air-dried for 5 minutes. All incubations were displayed on a Parafilm sheet with the coated side of grid facing the drop. Two grids were prepared under identical conditions for each EV sample. The sample was analyzed immediately with the transmission electron microscope JEOL JEM-2100F High Resolution EM-20023 (JEOL, Freising,
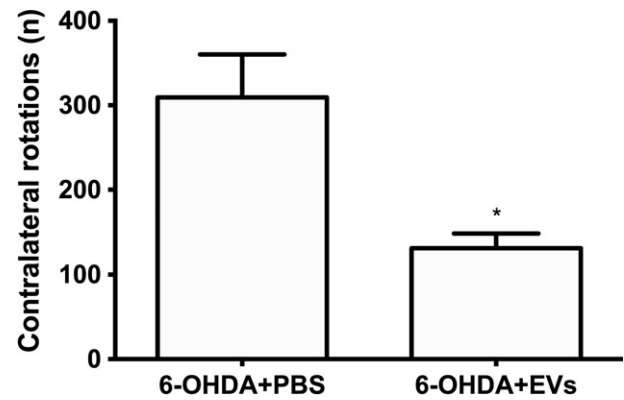

Figure 5. Effects of intranasally administered extracellular vesicles on 6-hydroxydopamine (6-OHDA)-lesioned rats' performance in the apomorphine (APO) test. APO was injected s.c. 5 minutes prior to the test, and rotations were counted for 30 minutes. Data represent mean + SEM values. Student's t test. *, $p \le .05$.

Germany) at 80 kV. The images were captured with a Olympus Quemesa camera, using the iTEM 5.2 software.

Protein Isolation and Western Blot Analysis

For preparation of total cell lysates, cell monolayers were washed twice with cold PBS, pH 7.3, and lysed in Pierce RIPA buffer supplemented with 1× Halt protease inhibitor cocktail for 15 minutes on ice. Samples were centrifuged at 14,000g for 30 minutes at 4°C. Supernatants derived after centrifugation of cellular lysates were aliquoted and kept at −20°C until analyzed. EVs were first precipitated in acetone (99.8%). Briefly, 1 volume of EV suspension was mixed with 4 volumes of −20°C acetone and incubated overnight at −20°C, then samples were centrifuged at 18,000g for 15 minutes at 4°C. Afterward, pellets were washed three times with acetone (80%). After acetone evaporation pellets were dissolved in Laemmli sample buffer, boiled and kept at −20°C until analyzed. Protein concentrations were measured with the NanoPhotometer Pearl (Implen, Munchen, Germany). For Western blot analysis cell and EV lysates diluted in a Laemmli sample buffer were heated for 5 minutes at 95°C. The same amounts of proteins from EVs and cellular lysates were loaded on Mini-PROTEAN TGX precast gels (Bio-Rad, Hercules, CA), subjected to electrophoresis in Mini-PROTEAN Tetra cell apparatus (Bio-Rad), then blotted onto a PVDF membrane in a semidry Trans-Blot Turbo transfer system (Bio-Rad) and blocked for 1 hour at room temperature with 5% BSA in PBS containing 0.18% Tween-20 (PBS-Tw). The membranes were then probed with primary antibodies against Syntenin-1, MFG-E8 and LGR5 for 1 hour at room temperature. Alternatively, membranes were incubated overnight with antibodies against HSP 70 at 4°C. After incubation with primary antibodies membranes were washed three times in PBS-Tw. After washing, membranes were incubated further with horseradish peroxidase-conjugated secondary antibody for 1 hour at room temperature.

Washing procedure was repeated and immunoreactive bands were detected with Clarity ECL Western blotting substrate (Bio-Rad) using ChemiDoc MP system (Bio-Rad).

LC–MS/MS Analysis

Sample proteins were reduced with 0.05 M Tris(2-carboxyethyl) phosphine hydrochloride (C4706, Sigma-Alrich) for 20 minutes at
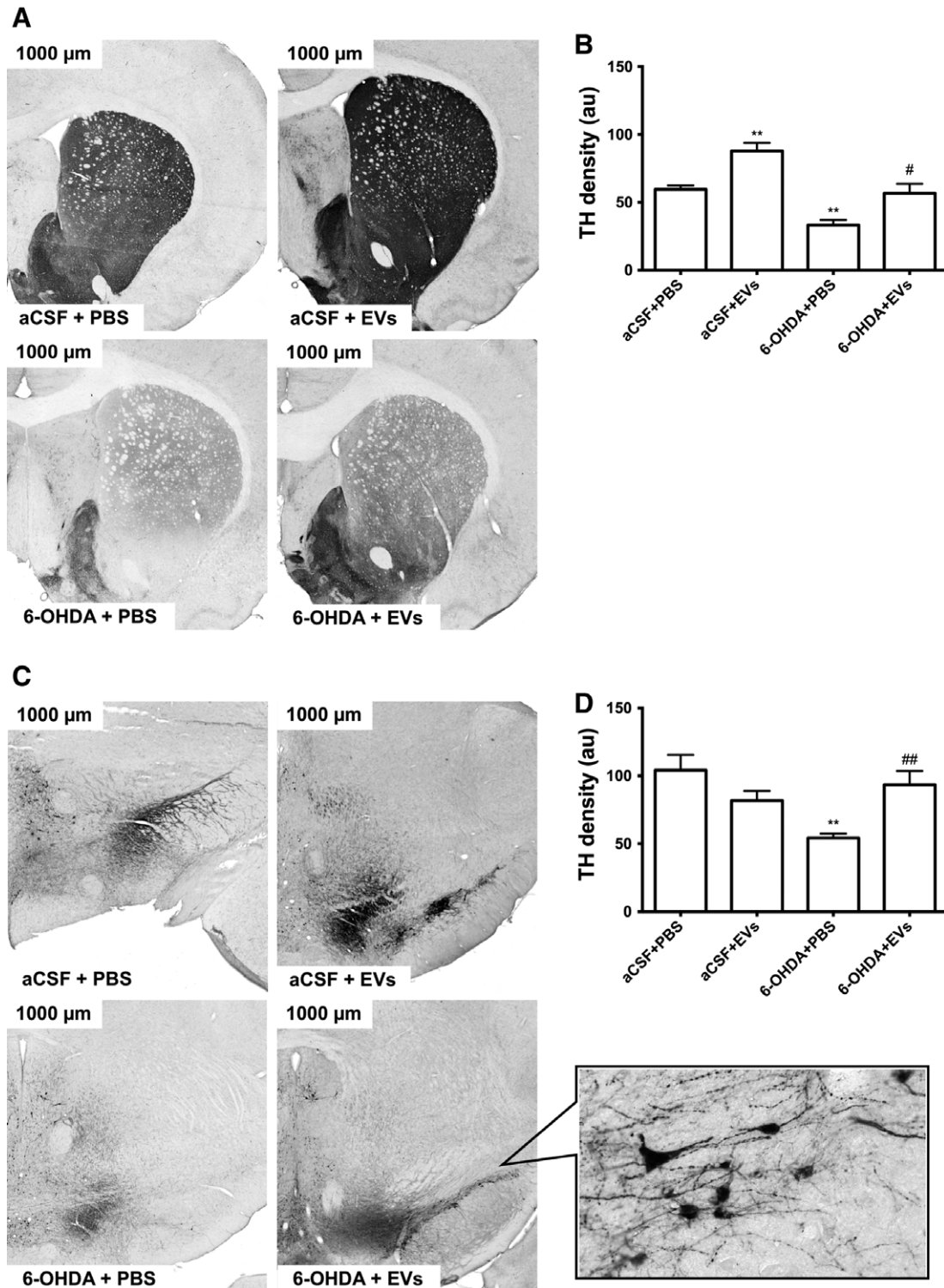
Figure 6. Influence of intranasally administered extracellular vesicles on expression of tyrosine hydroxylase in the substantia nigra (SN) and striatum of 6-OHDA-treated rats. Representative photographs show rat striatum **(A)** and SN **(C)** at ×300 magnification. Density measurements (a.u.) are shown in **(B)** for the striatum and in **(D)** for the SN. Inset of (C) depicts SN at higher magnification (×600). Values are expressed as mean ± SEM one-way ANOVA followed by Tukey's post-test. *, $p \le .05$ versus aCSF+PBS; #, $p \le .05$ versus 6-OHDA+PBS.

37°C and then alkylated with 0.15 M iodoacetamide (#57670 Fluka, Sigma-Alrich) at room temperature in the dark. Proteolysis was performed by adding 0.75 μg trypsin (Sequencing Grade Modified Trypsin, V5111, Promega, Madison, WI). After digestion peptides were purified with C18 microspin columns (Harvard Apparatus, Holliston, MA) according to manufacturer's protocol and redissolved in 30 μl of 50 mM NH_4HCO_3. Liquid chromatography coupled to tandem mass spectrometry (LC–MS/MS) analysis was carried out on an EASY-nLC (Thermo Fisher Scientific, Germany) connected to a Velos Pro-Orbitrap Elite

hybrid mass spectrometer (Thermo Fisher Scientific, Germany) with nanoelectrospray ion source (Thermo Fisher Scientific, Germany). The LC–MS/MS samples were separated using a 2-column setup consisting of on a 2 cm C18-A1 trap column (Thermo Fisher Scientific, Germany), followed by 10 cm C18-A2 analytical column (Thermo Fisher Scientific, Germany). The linear separation gradient consisted of 5% buffer B in 5 minutes, 35% buffer B in 60 minutes, 80% buffer B in 5 minutes and 100% buffer B in 10 minutes at a flow rate of 0.3 µl/min (buffer A: 0.1% TFA in 1% acetonitrile; buffer B: 0.1% TFA acid in 98% acetonitrile). Four microliters of sample was injected per LC–MS/MS run and analyzed. Full MS scan was acquired with a resolution of 60,000 at normal mass range in the orbitrap analyzer the method was set to fragment the 20 most intense precursor ions with CID (energy 35). Data was acquired using the LTQ Tune software. Acquired MS2 scans were searched against UniProt protein database using the Sequest search algorithms in Thermo Proteome Discoverer. Allowed mass error for the precursor ions was 15 ppm. And for the fragment in 0.8 Da. A static residue modification parameter was set for carbamidomethyl +57.021 Da (C) of cysteine residue. Methionine oxidation was set as dynamic modification +15.995 Da (M). Semitryptic peptides were allowed for scoring maximum of 2 missed cleavages were considered. LC–MS/MS analysis was performed at the Proteomics Unit, Institute of Biotechnology, University of Helsinki, Finland.

Statistical Analysis

Behavioral and immunohistochemical results are presented as the mean $\pm$ SEM. The behavioral data from apomorphine rotation test were analyzed by Student's t test. CatWalk data were analyzed by two-way analysis of variance (ANOVA) followed by Fisher's LSD post-test and quantitative immunohistochemical data—by one-way ANOVA followed by Tukey's post-test. Graph Pad Prism software version 6.0 (Graph Pad Software, Inc.) was used for data analysis. In all cases, a p value ≤.05 was taken as the criterion of statistically significant difference.

RESULTS

Identification of EV Proteins by LC–MS/MS

Total proteins extracted from EVs were digested with trypsin, and resultant peptides were subjected to LC–MS/MS analysis for protein identification. In total, we identified 80 proteins in EVs derived from SHED cultures (Supporting Information Table S1). The majority of the identified proteins are included in the vesiclepedia database [25].

Intranasal Administration of EVs Significantly Improved 6-OHDA-Induced Impairment of Gait Parameters

We did not observe gait impairments in the CatWalk training on day 7 after 6-OHDA injection (data not shown), whereas significant impairments were observed on postlesion day 20. Gait analysis showed significant interactions between groups in the following parameters: stand ($F_{7,184}$ = 15.12, $p \leq$ .0001, Fig. 3A), stride length ($F_{7,184}$ = 29.44, $p \leq$ .0001, Fig. 3B), step cycle ($F_{7,184}$ = 13.09, $p \leq$ .0001, Fig. 4A), and duty cycle ($F_{7,184}$ = 10.99, $p \leq$ .0001, Fig. 4B). Injection of 6-OHDA significantly prolonged the stand time of all paws ($p \leq$ .001, Fig. 3A) compared with the control group, whereas 6-OHDA group rats that received EVs treatment demonstrated significantly shorter stand time of the right hind

($p \leq$ .001) and left hind ($p \leq$ .001) paws (Fig. 3A). The 6-OHDA injection significantly decreased the stride length of the right front ($p \leq$ .01), right hind ($p \leq$ .05), left front ($p \leq$ .001), and left hind ($p \leq$ .05) paws (Fig. 3B). In the EV-treated 6-OHDA rats, stride length of the left front paw was significantly increased compared with the 6-OHDA group ($p \leq$ .01, Fig. 3B). 6-OHDA injection resulted in significantly longer step cycle of all paws ($p \leq$ .001 for the right front, right hind, and left hind, $p \leq$ .05 for the left front) compared with the control group (Fig. 4A). The 6-OHDA group rats showed an increase in the duty cycle of the right front ($p \leq$ .01), right hind ($p \leq$ .05), and left hind ($p \leq$ .01) paws (Fig. 4B). The EVs treatment reduced duty cycle parameter of the right front ($p \leq$ .05), right hind ($p \leq$ .01), and left hind ($p \leq$ .001) paws (Fig. 4B).

EVs Reduced Number of Apomorphine-Induced Contralateral Rotations

In the apomorphine rotation test, EV-treated 6-OHDA group rats demonstrated a significant decrease (2.2-fold) in the number of contralateral rotations compared with the 6-OHDA group (p = .02; Fig. 5).

Intranasal Administration of EVs Increased Expression of TH in the SN and Striatum of 6-OHDA-Treated Rats

Significant differences in TH density were observed between groups in the striatum ($F_{3,12}$ = 21.33, $p \leq$ .0001) and SN ($F_{3,14}$ = 5.8, p = .0086). Animals that received 6-OHDA injections demonstrated significant (approximately twofold) decrease in TH density in the striatum ($p \leq$ .05, Fig. 6A, 6B) and in the SN ($p \leq$ .01, Fig. 6C, 6D) compared with the controls. Treatment of 6-OHDA-injected rats with EVs increased TH density in the striatum ($p \leq$ .05, Fig. 6A, 6B) and in the SN ($p \leq$ .05, Fig. 6C, 6D) to the control levels. Administration of EVs per se significantly increased TH density in the striatum ($p \leq$ .01, Fig. 6A, 6B) but did not alter TH density in the SN.

DISCUSSION

PD is a progressive neurodegenerative disorder that starts from the deterioration of the nigro-striatal system, brain structures that control locomotion. This effect correlates with gait impairments and postural instability—the hallmark symptoms of PD. Numerous studies described strong correlation between abnormalities of locomotor parameters and loss of midbrain dopaminergic neurons [1, 26] that in turn, cause imbalance in other neurotransmitter systems [27]. To evaluate locomotor function in PD model we used rats with nigro-striatal lesion caused by injection of 6-OHDA into the MFB [28, 29]. The MFB model has been proven to be the most accurate to display gait changes and dopaminergic system damage specific to PD [28, 29]. According to the literature, motor impairments after 6-OHDA injection into the MFB can be detected as early as 1 week postlesion [26], fully develop after 3–4 weeks [21], and after 6 weeks DA cell loss reaches 88.79% [1, 26].

In our study, using computerized and automated CatWalk gait-analysis technique [21], we demonstrated that in 6-OHDA-treated rats the tested gait parameters were not significantly impaired on postlesion day 7, suggesting that nigro-striatal damage has not reached critical level for manifestation of motor dysfunction. Nevertheless, on postlesion day 20, all tested gait

parameters were significantly impaired in the 6-OHDA rats. These impairments were considerably reversed in 6-OHDA rats treated by EVs. The normalized stand (Fig. 3A), stride length (Fig. 3B), and step cycle (Fig. 4A) analyses indicated improved coordination and posture; animals felt more stable to walk and took a step significantly faster compared with 6-OHDA-lesion group rats. In addition, a decreased duty cycle (Fig. 4B) showed how freely animals crossed the walkway. Furthermore, EVs slowed down numbers of 6-OHDA-induced contralateral rotations in apomorphine test (Fig. 5). Importantly, motor improvements correlated with the rescue of TH expression in the SN and striatum of 6-OHDA-treated animals (Fig. 6). Therefore, we propose that EVs may protect dopamine-producing cells against 6-OHDA-induced neuronal death in the nigro-striatal pathways and slow down the progression of PD. These findings suggest that use of EVs during early clinical stages may represent a promising strategy against PD.

Another interesting finding of this study is that EVs per se increased (by approximately 30%) the expression of TH in the striatum (Fig. 6B), but not in the SN (Fig. 6D). At the same time, no influence of EVs on gait parameters in control group animals was observed (Figs. 3 and 4). These findings indicate that EVs may differentially affect dopaminergic neurons in the SN and their projections in the striatum, for example, by increased anterograde axonal transport, or decreased TH degradation in axonal terminals.

What could be the mechanism behind neuroprotective action of EVs? 6-OHDA-induced nigrostriatal damage is mainly the result of massive oxidative stress [30]. After injection, 6-OHDA is taken into the dopaminergic neurons by dopamine transporters, where it undergoes rapid auto-oxidation promoting formation of large amounts of reactive oxygen species [31]. 6-OHDA also accumulates in mitochondria and causes respiratory inhibition by blocking electron respiratory chains [32]. It is therefore plausible, that EVs exert their neuroprotective actions by reducing sensitivity of dopaminergic neurons to the 6-OHDA-induced oxidative stress. However, surprisingly little is known about antioxidative action of EVs in the CNS. In this study, we have used proteomic approach to explore cargo content of EVs (Supporting Information Tables S1 and S2). Among identified proteins was Cu/Zn superoxide dismutase 1 (SOD1), an enzyme converting harmful free superoxide radicals to molecular oxygen and hydrogen peroxide. It has been demonstrated, that SOD1 overexpression can rescue dopaminergic cells loss and prevent locomotor disabilities in a Drosophila model of PD [33]. EVs also contained antioxidant proteins thioredoxin (TXN) and peroxiredoxin-6 (PRDX6) which are important for the neutralization of hydrogen peroxide (Supporting Information Table S1). Therefore delivery of Cu/Zn SOD1, TXN and PRDX6 proteins by EVs may reduce sensitivity of dopaminergic neurons to the 6-OHDA-induced oxidative stress. Heat shock protein 70 (HSP70) is another regulator of cellular redox environment [34]. HSP70 gene transfer to dopamine neurons by adeno-associated virus (AAV) significantly protected mouse dopaminergic system against 1-methyl-4-phenyl-1,2,3,6-tetrahydropyridine (MPTP)-induced neurodegeneration [35] Knockdown of HSP70 in dopaminergic neurons of the SN caused neuronal death and multiple motor disturbances in rats, whereas enhanced expression of inducible HSP70 reversed neurodegeneration by increasing numbers of TH-positive neurons and preventing motor impairments [36]. HSP70 is an ubiquitous marker of EVs, therefore it could be important for the

neuroprotection against 6-OHDA-induced nigro-striatal destruction. Of note, EVs used in the present study were also HSP70-positive (Fig. 1B). Proteomic analysis also revealed the presence of dermcidin protein in EVs. (Supporting Information Table S1). HSP70 has been shown to bind specifically to amino-terminal sequence (CHEC-9) of dermcidin in vitro and in cerebral cortex after oral delivery in rats [37]. Furthermore, treatment with CHEC-9 increased HSP70-dependent dissolution α-synuclein aggregates [37]. Therefore, we suggest that dermcidin could potentially enhance therapeutic properties of exosomal HSP70. Adaptor protein 14-3-3ζ was also identified in EVs (Supporting Information Table S1). 14-3-3ζ binds and modulates activity of the target proteins by recognition of a phosphoserine or phosphothreonine motifs. Importantly, 14-3-3ζ is an endogenous activator of TH in midbrain dopaminergic neurons [38]. 14-3-3ζ may also reduce sensitivity of TH to the proteolysis [39] thereby increasing overall protein expression levels. Therefore, delivery of 14-3-3ζ proteins by EVs may be important for the normalization of TH expression in striatum and SN. Brain acid soluble protein 1 (BASP1) also known as CAP-23, or NAP-22 was identified with high level of confidence in the EVs derived from SHEDs (Supporting Information Table S1). BASP1 protein is regulator of neurite outgrowth and nerve regeneration [40]. Recent study demonstrated that calcineurin-dependent phosphorylation of BASP1 is critical for the restoration of dopamine trafficking at the presynaptic terminals and rescue of dopaminergic neurons in a rat model of α-synuclein-induced toxicity [41]. Another group of proteins identified in this study belong to a family of annexins. EVs were positive for annexin 1 (ANXA1), ANXA2, ANXA5, and ANXA6 (Supporting Information Table S1). Annexins are calcium-regulated membrane binding proteins participating in a number of cellular functions [42]. ANXA1 is known inhibitor of phospholipase A2 pathway blocking eicosanoid production and suppressing inflammatory response [43]. ANXA2 and ANXA5 have been shown to protect neuronal and glial cells of primary neocortical cultures against hypoxia and oxidative stress [44]. Therefore, we suggest that transport of annexins into the injured nigrostriatal tissues may represent an important mechanism of neuroprotective action of EVs. At present, it is unclear whether EVs increased TH expression in SN and striatum directly by affecting dopaminergic neurons, or indirectly via modulation of astroglial and microglial responses. Recent study demonstrated, that intranasally injected EVs accumulated in microglial cells and reduced inflammation in the hippocampal areas after induction of status epilepticus [10]. Another report showed that after traumatic brain injury EVs decreased secretion of IL-1β by the GFAP-positive astrocytes [11]. Therefore, accumulating evidence points to the pleiotropic effects of the EVs. We propose that EVs exert neuroprotective actions by simultaneous targeting of dopaminergic neurons and by possible modulation of astroglial and possibly microglial responses to the injury of nigro-striatal pathways.

CONCLUSION

We demonstrated, for the first time, the therapeutic efficacy of intranasal administration of EVs derived from SHEDs in rat model of PD induced by 6-OHDA intra-MFB lesion. We showed, that EVs can effectively reverse gait impairments and normalize TH expression in the SN and striatum. Our proof of concept study

demonstrates that EVs could be potentially exploited for the development of novel and minimally invasive therapies that delay progression of the disease and mitigate disability in PD patients.

AUTHOR CONTRIBUTIONS

K.N.: Concept and design, provision of study material, collection of data, data analysis and interpretation, manuscript writing; V.P.: Concept and design, provision of study material, collection of data, data analysis and interpretation; J.P.: Provision of study material, collection of data, participation in operations; Z.D.: Participation in operations and apomorphine test; U.J., A.J.: Collection and assembly of data; V.T.: Collection and assembly of data, data analysis and interpretation; K.K.: Collection and assembly of data; V.K.: Concept and design, Manuscript writing, Final approval of manuscript; B.J.: Administrative support, participation in apomorphine test; A.P.: Concept and design, data analysis and interpretation, manuscript writing, final approval of manuscript, overall coordination of the project.

DISCLOSURE OF POTENTIAL CONFLICTS OF INTEREST

The authors indicated no potential conflicts of interest.

REFERENCES

1 Shulman JM, De Jager PL, Feany MB. Parkinson's disease: Genetics and pathogenesis. Annu Rev Pathol 2011;6:193–222.

2 Cheng HC, Ulane CM, Burke RE. Clinical progression in Parkinson disease and the neurobiology of axons. Ann Neurol 2010;67:715–725.

3 Kirkeby A, Grealish S, Wolf DA et al. Generation of regionally specified neural progenitors and functional neurons from human embryonic stem cells under defined conditions. Cell Rep 2012;1:703–714.

4 Kriks S, Shim JW, Piao J et al. Dopamine neurons derived from human ES cells efficiently engraft in animal models of Parkinson's disease. Nature 2011;480:547–551.

5 Barker RA, Parmar M, Studer L et al. Human trials of stem cell-derived dopamine neurons for Parkinson's disease: Dawn of a new era. Cell Stem Cell 2017;21:569–573.

6 Kourembanas S. Exosomes: Vehicles of intercellular signaling, biomarkers, and vectors of cell therapy. Annu Rev Physiol 2015;77:13–27.

7 Maas SLN, Breakefield XO, Weaver AM. Extracellular vesicles: Unique intercellular delivery vehicles. Trends Cell Biol 2017;27:172–188.

8 Alvarez-Erviti L, Seow Y, Yin H et al. Delivery of siRNA to the mouse brain by systemic injection of targeted exosomes. Nat Biotechnol 2011;29:341–345.

9 Yang T, Martin P, Fogarty B et al. Exosome delivered anticancer drugs across the blood-brain barrier for brain cancer therapy in *Danio rerio*. Pharm Res 2015;32:2003–2014.

10 Gyorgy B, Hung ME, Breakefield XO et al. Therapeutic applications of extracellular vesicles: Clinical promise and open questions. Annu Rev Pharmacol Toxicol 2015;55:439–464.

11 Long Q, Upadhya D, Hattiangady B et al. Intranasal MSC-derived A1-exosomes ease inflammation, and prevent abnormal neurogenesis and memory dysfunction after status epilepticus. Proc Natl Acad Sci USA 2017;114:E3536–E3545.

12 Kim DK, Nishida H, An SY et al. Chromatographically isolated CD63+CD81+ extracellular vesicles from mesenchymal stromal cells rescue cognitive impairments after TBI. Proc Natl Acad Sci USA 2016;113:170–175.

13 Haney MJ, Zhao Y, Harrison EB et al. Specific transfection of inflamed brain by macrophages: A new therapeutic strategy for neurodegenerative diseases. PLoS One 2013;8:e61852.

14 Sun D, Zhuang X, Xiang X et al. A novel nanoparticle drug delivery system: The anti-inflammatory activity of curcumin is enhanced when encapsulated in exosomes. Mol Ther 2010;18:1606–1614.

15 Kaukua N, Shahidi MK, Konstantinidou C et al. Glial origin of mesenchymal stem cells in a tooth model system. Nature 2014;513:551–554.

16 Sakai K, Yamamoto A, Matsubara K et al. Human dental pulp-derived stem cells promote locomotor recovery after complete transection of the rat spinal cord by multiple neuro-regenerative mechanisms. J Clin Invest 2012;122:80–90.

17 Jarmalaviciute A, Tunaitis V, Strainiene E et al. A new experimental model for neuronal and glial differentiation using stem cells derived from human exfoliated deciduous teeth. J Mol Neurosci 2013;51:307–317.

18 Fujii H, Matsubara K, Sakai K et al. Dopaminergic differentiation of stem cells from human deciduous teeth and their therapeutic benefits for Parkinsonian rats. Brain Res 1613; 2015:59–72.

19 Martens W, Sanen K, Georgiou M et al. Human dental pulp stem cells can differentiate into Schwann cells and promote and guide neurite outgrowth in an aligned tissue-engineered collagen construct in vitro. FASEB J 2014;28: 1634–1643.

20 Jarmalaviciute A, Tunaitis V, Pivoraite U et al. Exosomes from dental pulp stem cells rescue human dopaminergic neurons from 6-hydroxy-dopamine-induced apoptosis. Cytotherapy 2015; 17:932–939.

21 Zhou M, Zhang W, Chang J et al. Gait analysis in three different 6-hydroxydopamine rat models of Parkinson's disease. Neurosci Lett 2015;584:184–189.

22 Hamers FP, Koopmans GC, Joosten EA. CatWalk-assisted gait analysis in the assessment of spinal cord injury. J Neurotrauma 2006;23:537–548.

23 Gabriel AF, Marcus MA, Honig WM et al. The CatWalk method: A detailed analysis of behavioral changes after acute inflammatory pain in the rat. J Neurosci Methods 2007;163:9–16.

24 Thery C, Amigorena S, Raposo G et al. Isolation and characterization of exosomes from cell culture supernatants and biological fluids. Curr Protoc Cell Biol 2006.

25 Kalra H, Simpson RJ, Ji H et al. Vesiclepedia: A compendium for extracellular vesicles with continuous community annotation. PLoS Biol 2012;10:e1001450.

26 Boix J, von Hieber D, Connor B. Gait analysis for early detection of motor symptoms in the 6-OHDA rat model of Parkinson's disease. Front Behav Neurosci 2018;12:39.

27 Henning J, Strauss U, Wree A et al. Differential astroglial activation in 6-hydroxydopamine models of Parkinson's disease. Neurosci Res 2008;62:246–253.

28 Boix J, Padel T, Paul G. A partial lesion model of Parkinson's disease in mice— Characterization of a 6-OHDA-induced medial forebrain bundle lesion. Behav Brain Res 2015; 284:196–206.

29 Ma Y, Zhan M, OuYang L et al. The effects of unilateral 6-OHDA lesion in medial forebrain bundle on the motor, cognitive dysfunctions and vulnerability of different striatal interneuron types in rats. Behav Brain Res 2014;266:37–45.

30 Blandini F, Armentero MT, Martignoni E. The 6-hydroxydopamine model: News from the past. Parkinsonism Relat Disord 2008;14: S124–S129.

31 Schober A. Classic toxin-induced animal models of Parkinson's disease: 6-OHDA and MPTP. Cell Tissue Res 2004;318:215–224.

32 Mazzio E, Reams R, Soliman K. The role of oxidative stress, impaired glycolysis and mitochondrial respiratory redox failure in the cytotoxic effects of 6-hydroxydopamine in vitro. Brain Res 2004;1004:29–44.

33 Botella JA, Bayersdorfer F, Schneuwly S. Superoxide dismutase overexpression protects dopaminergic neurons in a Drosophila model of Parkinson's disease. Neurobiol Dis 2008;30: 65–73.

34 Calabrese V, Cornelius C, Cuzzocrea S et al. Hormesis, cellular stress response and vitagenes as critical determinants in aging and longevity. Mol Aspects Med 2011;32:279–304.

35 Dong Z, Wolfer DP, Lipp HP et al. Hsp70 gene transfer by adeno-associated virus inhibits MPTP-induced nigrostriatal degeneration in the mouse model of Parkinson disease. Mol Ther 2005;11:80–88.

36 Ekimova IV, Plaksina DV, Pastukhov YF et al. New HSF1 inducer as a therapeutic agent

in a rodent model of Parkinson's disease. Exp Neurol 2018;306:199–208.

37 Cunningham TJ, Greenstein JI, Loewenstern J et al. Anti-inflammatory peptide regulates the supply of heat shock protein 70 monomers: Implications for aging and age-related disease. Rejuvenation Res 2015;18:136–144.

38 Wang J, Lou H, Pedersen CJ et al. 14-3-3zeta contributes to tyrosine hydroxylase activity in MN9D cells: Localization of dopamine regulatory proteins to mitochondria. J Biol Chem 2009;284:14011–14019.

39 Obsilova V, Nedbalkova E, Silhan J et al. The 14-3-3 protein affects the conformation of the regulatory domain of human tyrosine hydroxylase. Biochemistry 2008;47:1768–1777.

40 Korshunova I, Caroni P, Kolkova K et al. Characterization of BASP1-mediated neurite outgrowth. J Neurosci Res 2008;86:2201–2213.

41 Caraveo G, Soste M, Cappelleti V et al. FKBP12 contributes to alpha-synuclein toxicity by regulating the calcineurin-dependent phosphoproteome. Proc Natl Acad Sci USA 2017; 114:E11313–E11322.

42 Mirsaeidi M, Gidfar S, Vu A et al. Annexins family: Insights into their functions and potential role in pathogenesis of sarcoidosis. J Transl Med 2016;14:89.

43 Perretti M, D'Acquisto F. Annexin A1 and glucocorticoids as effectors of the resolution of inflammation. Nat Rev Immunol 2009; 9:62–70.

44 Han S, Zhang KH, Lu PH et al. Effects of annexins II and V on survival of neurons and astrocytes in vitro. Acta Pharmacol Sin 2004;25:602–610.

See www.StemCellsTM.com for supporting information available online.